W. Serbiński, J. I. Łubiński, K. Druet
Gdańsk University of Technology, Faculty of Mechanical Engineering, Poland

MICROSTRUCTURE AND WEAR OF CAST ALUMINIUM ALLOY WITH LASER MODIFIED SURFACE LAYER

ABSTRACT

The main reason for laser surface modification of the components such as pistons and cylinder blocks made of cast aluminium alloys is to obtain high hardness and wear resistance at the working surface for larger lifetime as a result of the rapid solidification. The final microstructure, phase composition and properties of aluminium alloys depend on the laser process parameters and obviously on the nature of the equilibrium system aluminium alloys. The effect of laser surface remelting at cryogenic conditions on the microstructure, microhardness and wear characteristics of AlSi13Mg1CuNi alloy are presented. The beneficial effect of laser treatment on the microstructure, microhardness and wear behaviour of the cast aluminium alloy were observed.

Key words: *aluminium alloy, laser technology, microstructure, sliding friction, wear*

INTRODUCTION

The following processes have been developed for laser modification of aluminium surface: surface melting [1], surface alloying [2, 3], cladding [4, 5] and amorphisation [6]. It is especially marked in the case of light alloys such as aluminium-silicon alloys that are widely used as casting alloys in the automobile or aeronautic units [7, 8]. In cast materials, surface remelting eliminates casting defects (e.g., porosity, cold shuts). However, the main reason for surface laser melting on components made of aluminium alloys is to increase hardness and wear resistance at the surface for extended lifetime as a result of the rapid solidification. The final microstructure and properties of aluminium alloys depend on the laser process parameters. Quenching rate, solidification rate and temperature gradient influence mainly the solidification behaviour. The temperature gradient in laser surface melting depends on the energy density and the solidification rate, and apart from stationary pulsing, on the displacement rate [9]. The laser surface melting at room conditions produces a very fine eutectic on the surface of both modified and unmodified Al-Si alloys [10, 11, 12]. The aim of this paper is performance the effect of laser surface remelting at cryogenic conditions on microstructure, microhardness and wear characteristics of the casting alloy AlSi13Mg1CuNi.

EXPERIMENTAL DETAILS

The processed material (AlSi13Mg1CuNi alloy) was immersed in liquid nitrogen and irradiated by a scanning CO_2 laser allowing for the treatment of the entire specimen surface in multiple passes. The material was processed in batches, each at different laser beam power and shape settings and different scanning velocities [13-15]. In order to improve the efficiency of laser

radiation absorption and decrease the exposure of the scanning laser head to reflected radiation the surface was covered with a layer of absorbent.
Several settings were used for surface processing of laser power and beam shape, scanning velocity, and the thickness of the raw material. In Table 1 a detailed description is given of the conditions of laser processing of the AlSi13Mg1CuNi alloy.

Table 1. *Laser processing conditions used for the AlSi13Mg1CuNi alloy at cryogenic conditions*

Specimen code marking	Laser processing conditions				Raw material thickness [mm]
	Laser beam dimensions [mm]	Laser beam power [kW]	Scanning velocity [m/min]	Scanning stroke [mm]	
101, 130	Ø 3	1,5	0,5	1	13
300, 330	Ø 3	1,5	1,0	1	13
112	1x20	6,0	1,0	10	13
023, 21 B	1x20	5,0	1,0	10	13
081	1x20	4,0	1,0	10	13
005	1x20	5,0	1,0	10	7
118	1x20	4,0	1,0	10	7
004	Ø 3	1,5	0,5	1	7

The samples were manipulated with an X-Y stage where movement was controlled by a computer at a speed of 1,7 $mm \cdot s^{-1}$. For microstructure, hardness and wear investigations samples were prepared with overlapping scanned surface.

RESULTS AND DISCUSSION

The surface microstructure and fracture observations before and after laser treatment of AlSi13Mg1CuNi alloy were provided using of the Scanning Electron Microscope (SEM).
The morphology of AlSi13Mg1CuNi alloy before and after laser treatment at cryogenic conditions are compared at microscopic scale. Fig. 1a shows the SEM surface microstructure of the AlSi13Mg1CuNi alloy, which was laser remelted at cryogenic conditions without scan lines overlap.
The layers produced by laser remelting have a smooth surface, exhibit a dense, pore-free cast structure. Fig. 1b shows that the fracture of the sample occurred perpendicular to the direction of laser scanning. It is found that the layer (Fig. 1b) remelted by laser beam (thickness 0,663 mm) consists of two zones, which structure and thickness are diverse and depend mainly on melting and solidification rate and temperature gradient.
Fig. 2a shows the ductile fracture in the first remelted zone of the layer. Ultra-fine intermetallic compounds in the matrix of this zone were found. The base AlSi13Mg1CuNi alloy demonstrates generally brittle transcrystalline fracture (Fig. 2b). If the silicon phase is coarse and acicular, the Al-Si alloys exhibit crack sensitivity. Therefore, these alloys should be modified to improve their mechanical properties.

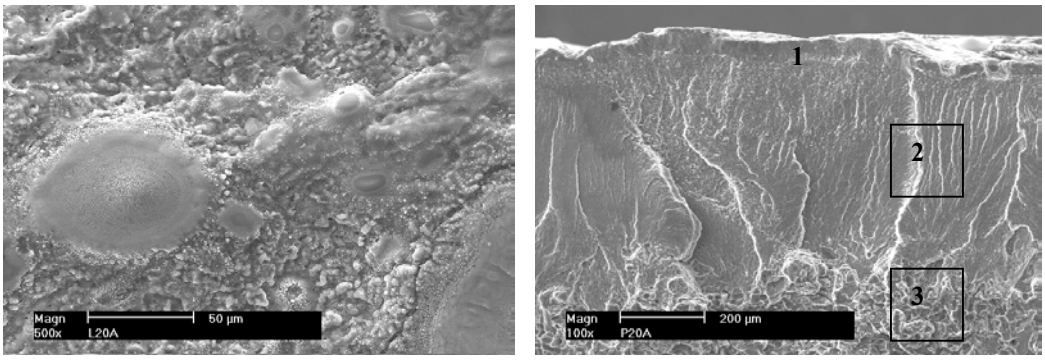

a) b)

Fig. 1. View (SEM) of the AlSi13Mg1CuNi alloy remelted by laser beam ∅ 3mm/1500W (material code 330) at cryogenic conditions; a) – surface, b) – fracture

Fig. 3 shows the distributive relations of microhardness with distance from the outer edge cross-section of the laser remelted AlSi13Mg1CuNi alloy. It is seen that the microhardness of the laser-remelted region is considerably higher than that base material and the highest hardness is localized on the surface of the specimen. These results well correspond with ultra-fine microstructure observed in the first remelted zone (Fig. 2a).

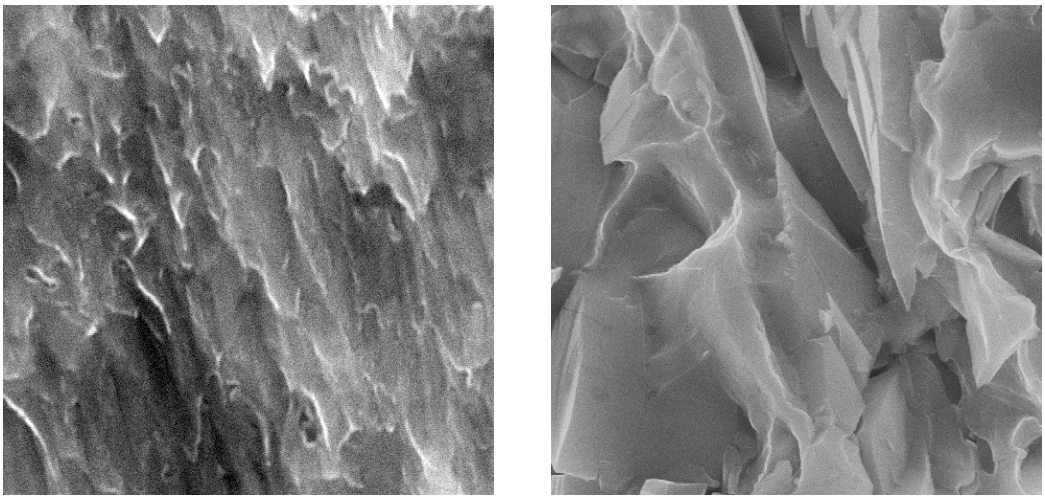

a) b)

Fig. 2. Fracture (SEM) of the laser remelted AlSi13Mg1CuNi alloy (material code 330): a) – ductile in first zone, b) – brittle in base material

The microhardness of substrate and laser remelted at cryogenic conditions regions were measured on cross-section using a PMT-3 tester with a Vickers diamond indenter under a 50 grams load applied during 15 s. All reported values represent the average and standard deviation of six replicates.

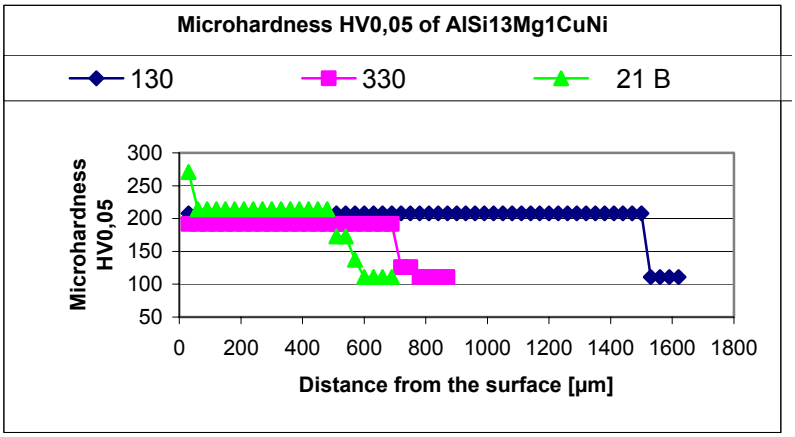

Fig. 3. Distribution of the microhardness with distance from the outer edge cross-section of the laser remelted AlSi13Mg1CuNi alloy. Material code: 130, 330, 21 B

As a result of the laser processing applied a favourable decrease in grain size is achieved in the surface layer of the material. Also are observed changes in alloy components distribution along perpendicular to the surface. Furthermore, the nanocrystalline structures are observed in the remelted surface layer of AlSi13Mg1CuNi alloy. As a result of the combined effect of structural changes in the remelted layer a compressive stress is introduced. The microhardness is thus increased from 110 HV0,05 to 260 HV0,05.

Tribological investigations were performed by means of the PTZ – 1 tribometer. The PTZ – 1 tribometer has been designed for tests on sliding pairs in reciprocating motion, especially such pairs as piston and cylinder liner in a piston machines e.g. internal combustion engines. The stand design has been described in detail in earlier papers [16-19]. Counter specimens were machined from cast iron – 300 grade (PN), equivalent to GG30 (DIN). The working surfaces were polished to a final roughness of $R_a = 0{,}32$ µm.

A schematic of the sliding contact between the specimen and counter specimen is presented in Fig. 4. Heat transported to or from the chamber via the semiconductor elements is transferred from or to ambient through a large finned radiator integrated with the slider body. Air is forced through the radiator by a fan.

Sliding velocity is controlled by the computer also used to gather data. Load is set manually prior to the test. The computer also modulates the rotational velocity of the engine, so that the sliding velocity is not sinusoidally variable, but constant over more than 50% of the stroke length. The following principle variables were measured and data recorded:

- the sum of linear wear of the specimen and counter - specimen
- temperatures of specimen, counter – specimen and lubricant
- friction force
- horizontal and vertical displacement of the specimen (upper one)
- position of the slider

In Fig. 4a schematic of the sliding pair is presented. The top specimen (1), made of AlSi13Mg1CuNi alloy, is attached to a plunger which possesses only one degree of freedom (translation in vertical direction); The specimen working face is in contact with the surface of the counter specimen (2), made of 300 grade cast iron. The sliding pair is pressed together by the action of the plunger. The arrows indicate the direction and orientation of load (P) and the velocity of the reciprocating motion (V) of the counter specimen.

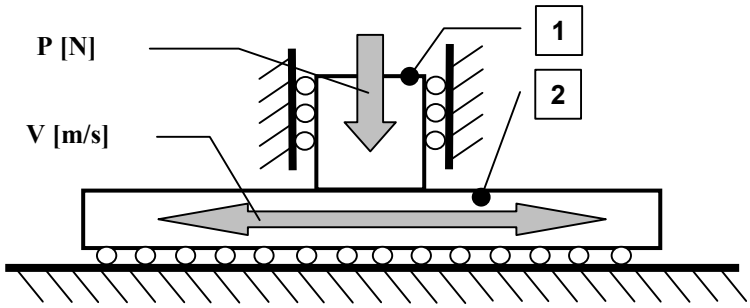

Fig. 4. Schematic of the reciprocating sliding friction contact between the aluminium specimen (1) and cast iron counter - specimen (2) on TPZ-1 reciprocating tribometer

In Fig. 5a photograph is presented of the laser processed face of the AlSi13Mg1CuNi alloy specimen (1) and the working face of the cast iron counter specimen (2) bearing a wear scar created during a test of the sliding pair on the TPZ-1 tribometer.

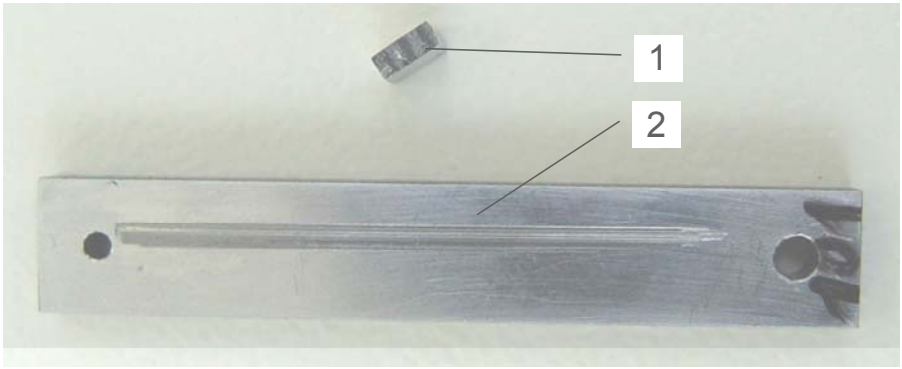

Fig. 5. AlSi13Mg1CuNi aluminium alloy specimen (1) and 300 grade cast iron counter – specimen (2) after testing on TPZ-1 tribometer. A view of the working surfaces of the specimens. Material code 101

The test were carried out with the use of a Petro-Oil Selektol Special 20W/40 (API SD) motor oil made by Orlen Oil Co. Ltd. The sliding pair was immersed in the oil bath.
The test were carried out under the following conditions:

- mean surface pressure: constant, 10 MPa, (100 N on a surface area of 10 mm^2)
- sliding velocity: constant (except dead centres), 0,1 ±0,02 m/s,
- lubricant bath temperature: constant, 70 ± 5 °C.

Prior to testing the sliding pair, specimen holders and the lubricant container were washed in petroleum spirit and later in acetone. The assembled test set up was filled with oil and heated to the desired test temperature.
Each test lasted 9 hours altogether. The test was divided into segments: the first 4 hours fo the test into four 30 minutes sections, and the remaining 5 hours into 1 hour sections. After each section the counter specimen was removed from its holder and a profile of the surface was taken. Thanks to the design of the TPZ-1 tribometer the counter specimen may be removed from its holder and then re – attached to the holder without changing its working position afterwards.

The surface profiles were taken with the use of a computerised profilographometer. The profile was taken in five passes across the wear scar and a single pass along the wear scar. The measurement was recorded in digital form for further processing.
During the test also are measured and recorded the displacements of the slider, loading force, friction force and the temperature of both specimens and the overall linear wear of the sliding pair.
The counter specimen surface profiles were used to evaluate the depth of the wear scar developed on the working surface of the counter specimen. Results are recorded in text files.
The files contain arrays of numbers corresponding to the values of maximum scar depths measured in subsequent test segments. A bitmap picture is also generated containing a composite graph of all the profiles, such as the graph presented in Fig. 6. The horizontal axis represents the length along the counter specimen surface (in mm) and the vertical axis the depth of the wear scar (in μm).

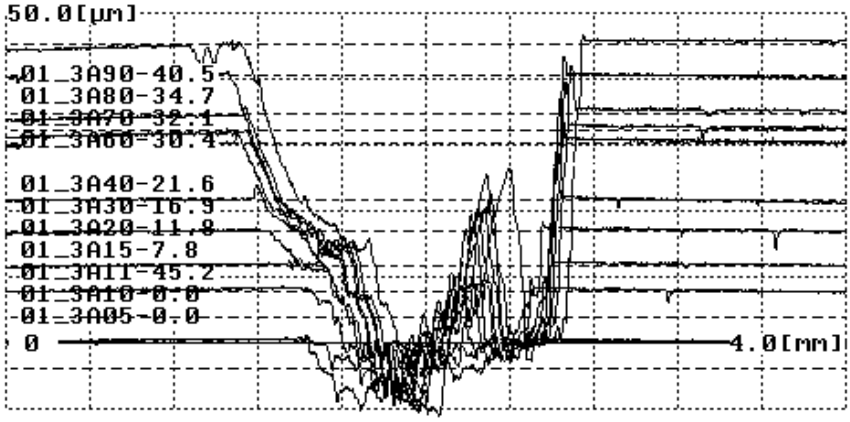

Fig. 6. A composite graph of 11 cross – sectional profiles of the wear scar on the cast iron counter – specimen. Profiles taken after subsequent time segments of a test carried out on material 101

It is worthy to note, that the general shape of the groove (wear scar) left on the counter specimen is similar for all the profiles shown. This is the result of a very slow rate of wear of the laser modified AlSi13Mg1CuNi alloy specimen. The face of the specimen was not changed noticeably during the test.
The continuous measurement of the overall wear of both the specimens and the cyclic measurement of the wear scar profile allows to distinguish the wear of the aluminium specimen from the wear of the counter specimen. Direct measurement of wear of the aluminium specimen is very difficult due to small size of the aluminium specimen and a complicated holder, which does not allow for correct re – seating of the specimen.
In Fig. 7 combined wear graphs for all the tested sliding pairs are presented as a function of the sliding distance. The curves in the left hand side graph (a) represent the overall wear of both the components of the sliding pair. The curves on the right hand side graph (b) represent the depth of the wear mark created in the surface of the counter specimen. As can be seen in both graphs the course of wear of both the components of the sliding pair differs with regard to the settings of the laser modification process. Under the same test conditions there are significant differences in wear of sliding pairs comprising AlSi13Mg1CuNi alloy specimens laser processed in different conditions.

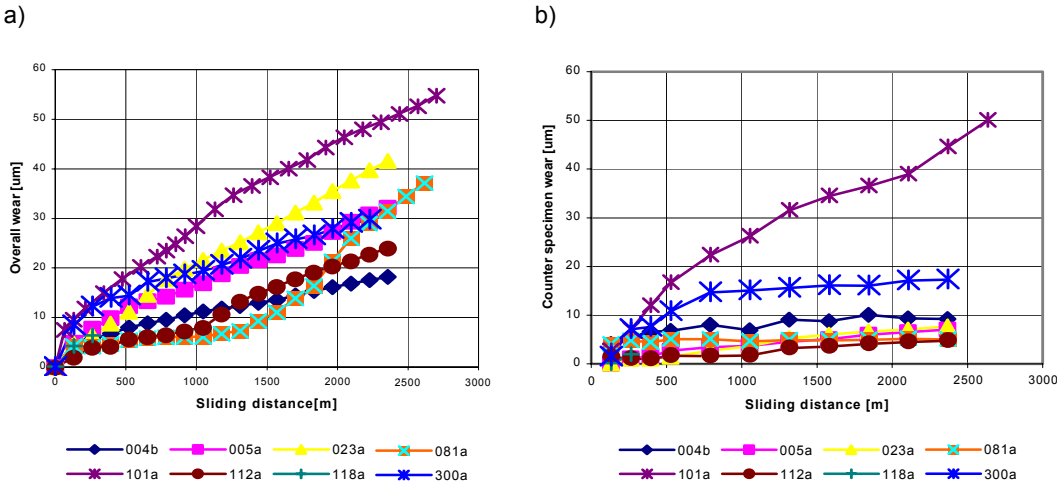

Fig. 7. Wear curves as a function of the sliding distance for all the tested material pairs. Overall wear of the sliding pair (a) and the wear of the cast iron counter specimen (b)

In order to show in more detail the nature of wear kinetics differences encountered, two more comparative graphs are presented in Fig. 8 in which two examples of wear test results are presented. In graphs a) and b) overall wear of the sliding pair and the wear of the counter specimen obtained for specimens coded 101 and 081 respectively are presented jointly.

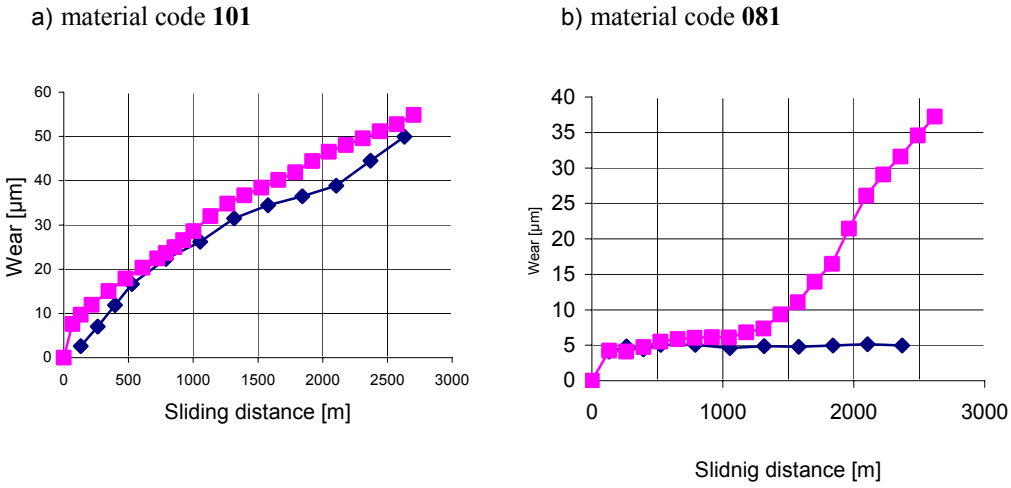

Fig. 8. Graphical representation of overall wear (■) and the wear of the cast iron counter-specimen (♦) for materials 101 (graph a) and 081 (graph b)

In graph a) the curves have very similar shapes and the values of wear for corresponding values of the sliding distance are almost identical for both curves, which indicates, that most of the wear is associated with the creation of the wear scar in the cast – iron counter specimen. Thus it can be stated, that the aluminium specimen coded 101 exhibited high resistance to wear in given test conditions at the cost of an increased wear of the counter specimen. In graph b) the results are completely different. The wear curve obtained for the counter – specimen exhibits wear from 0 to about 5 μm only during the initial 200 m of sliding distance; Over the remaining distance of more than 2000 m no wear increase can be observed. The wear of the 081 coded aluminium specimen 'follows' the wear of the counter – specimen over the initial 1000 m of the sliding distance, after exceeding which the rate of wear increases sharply with no changes in the counter – specimen wear.

As can be seen the sliding pair comprising the AlSi13Mg1CuNi alloy specimen coded 101 exhibits wear resistance superior to the pair comprising the specimen coded 081. On the other hand it is also clear, that the counter specimen wear rate is greater if coupled with a specimen coded 101 then with the specimen coded 081.

On the basis of the applied load and recorded friction force it was possible to establish the values of friction coefficient. The velocity of sliding varies in every cycle as the motion is reciprocating, thus in order to gather data for comparison of the friction coefficient between different sliding pairs the average friction coefficient was calculated for each part of the stroke during which the velocity was stabilized. From these values average friction coefficient was calculated for each segment of the test.

The calculated friction coefficients for sliding pairs with specimens coded 081 and 101 are presented in Fig. 9 as a function of the sliding distance. A slight chaotic variation of the friction coefficient magnitude is visible during the initial 1600 m of sliding distance. Further into the test the friction coefficient calculated for the pair comprising specimen coded 081 increases (from about 0.1 to about 0.13) at the same sliding distance the friction coefficient for the pair comprising material 101 the friction coefficient decreases (from about 0.09 to about 0.06). At the end of the test coefficients of friction are almost equal (with the value of about 0.11) for both the tested sliding pairs. Currently it is not known what is the specific reason for the described changes of friction coefficient and whether they are related to the observed changes in wear rate.

The results from friction coefficient measurements carried out on other sliding pairs are also inconclusive and require further studies.

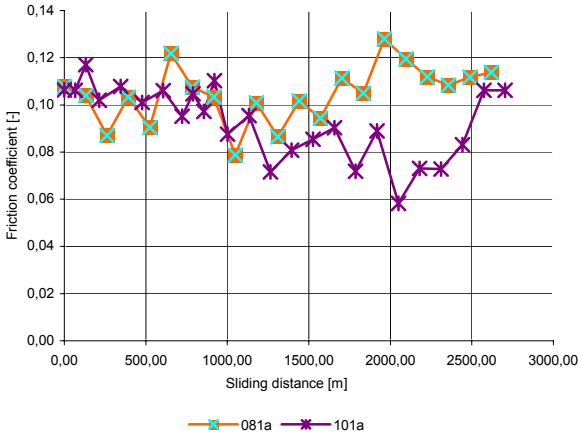

Fig. 9. Average friction coefficient versus sliding distance for materials 081 and 101

CONCLUSIONS

1. Layers of specified microstructure possessing significant thickness and relatively high hardness can be obtained on the surface of cast AlSi13Mg1CuNi alloy substrate by laser treatment at cryogenic conditions.
2. The layers have dense and porosity free structure.
3. The fine-crystalline of eutectic microstructure is the main factor affecting the specific microhardness and corrosion characteristics of these layers.
4. The microhardness of the layers on the surface of AlSi13Mg1CuNi alloy remelted at cryogenic conditions can reach 260 HV 0.05, much higher than the hardness of the base material (110 HV0.05).
5. As a result of tribological research carried out on sliding pairs composed of a laser modified AlSi13Mg1CuNi alloy and 300 grade (PN) cast iron it was established, that significant differences in wear behaviour can be observed in relation to the conditions of laser processing of the aluminium alloy specimens.
6. The kinetics of wear has been recorded for each of the sliding pairs comprised of specimens processed in different conditions. Also the course of changes of friction coefficient for each pair was established as a function of sliding distance. No relation between the friction coefficient changes and wear rate could be established as yet.
7. The experimental results indicate clearly an influence of the laser modification conditions of the aluminium alloy surface and wear resistance, which will be further used to perfect the technology to the level of industrial feasibility.
8. The TPZ – 1 tribometer and the methodology of tests and data processing proved in practice to be a useful tool for friction and wear testing in reciprocating sliding.

REFERENCES

1. Watkins K. G., K, Mc Mahon M. A., W. M. Steen W. M.: Materials Science and Engineering, A231 (1997, pp. 55-61.
2. Mordike B. L., Veit S.: ECLAT'88, Düsseldorf: DVS (1988), pp. 95-96
3. Das A. G., Paradkast D. K, Mishra R. S.: Scripta Metallurgica et Materialia, 26 (1992) p. 1211.
4. Nowotny S., Richter A., Tangermann K.: Journal of Thermal Spray Technology, Vol 8 (2) June (1999) pp. 258-262.
5. Ueniski K., Kabayashi K. F.: Intermetallics, 7 (1999) pp. 553-559.
6. Sordelet D. J., Besser M. F., Logsdon J. L.: Materials Science and Engineering, A255 (1998) pp. 54-65.
7. Tomlinson W. J., Bransden W. A. S.: Wear, 185 (1995) pp. 56-65.
8. Pei Y. T., De Hosson J. T. M.: Acta Metallurgica, 48 (2000) pp. 2617-2624.
9. Coriell S. R., Skeralka R. F.: Rapid Solidification Processing, Principles and Technology I, Baton Rouge, LA : Claitors (1980) pp. 35-49.
10. Bergmann H. W., Barton G., Mordike B. L., Fritsch H. U.: Rapidly Solidified Metastable Materials, Amsterdam, Elsevier (1984) pp. 28-29.
11. Hegge H. J., De Hosson J. T. M.: Scripta Metallurgica et Materialia, 24 (1990) p. 293.
12. Timsit R. S., Lauzon D. C.: J. Mater. Res., Vol. 9, n° 3, (1994) pp. 531-534.

13. Serbiński W.: The method and results of the laser surface treatment of aluminium alloys at cryogenic temperature. Polish J. Inżynieria Materiałowa, nr 6, (119) (2000), pp. 434-4437.
14. Serbiński W., Olive J.M., Frayret J.P., Morphology and corrosion characteristics of laser surface remelted Al-Si alloy at cryogenic conditions. Materials and Corrosion n° 53, 2002, pp. 335-340.
15. Serbiński W., Olive J.M., Wierzchoń T., Rudnicki J.: Study on the Surface Layers Created on Aluminium-silicon Alloy by Laser Treatment under Cryogenic Conditions, 3rd International Conference on Surface Engineering, Chengdu, P. R. China 2002, pp. 403-406.
16. Druet K., Łubiński J. I., Grymek S.: Stanowisko do badania tarcia ślizgowego w ruchu posuwisto-zwrotnym. J. of KONES 2002 vol. 9 nr 1-2 s. 72-79.
17. Druet K.: Urządzenie do badania tarcia ślizgowego w ruchu prostoliniowym. XXIII Jesienna Szkoła Tribologiczna – Kształtowanie tribologicznych właściwości wezłów tarcia. Teoria i praktyka. Zielona Góra -Lubiatów, wrzesień 1999, s. 29-34.
18. Druet K., Król M.: Tribometr TPZ. III Międzynarodowe Sympozjum INSYCONT. Materiały. Wydawnictwo AGH, Kraków 1990, s. 617-621.
19. Druet K., Łubiński T., Łubiński J. I.: Reciprocating motion tribometer. Abstracts of papers from 2nd World Tribology Congress. Vienna, Austria, 3-7 September 2001, s. 663